

PAPER • OPEN ACCESS

# Artificial Neural Network Modeling of Liquid Thermal Conductivity for alkanes, ketones and silanes

To cite this article: G Latini *et al* 2017 *J. Phys.: Conf. Ser.* **923** 012054

View the [article online](#) for updates and enhancements.

## Related content

- [Application of Artificial Neural Networks in the Heart Electrical Axis Position Conclusion Modeling](#)  
L N Bakanovskaya
- [Artificial neural networks with an infinite number of nodes](#)  
K Blekas and I E Lagaris
- [Application of artificial neural network for prediction of marine diesel engine performance](#)  
C W Mohd Noor, R Mamat, G Najafi et al.

# Artificial Neural Network Modeling of Liquid Thermal Conductivity for alkanes, ketones and silanes

G Latini<sup>1</sup>, G Di Nicola<sup>1</sup>, M Pierantozzi<sup>2</sup>, G Coccia<sup>1</sup> and S Tomassetti<sup>1</sup>

<sup>1</sup> DIISM, Università Politecnica delle Marche, Ancona, Italy

<sup>2</sup> SAAD, Università di Camerino, Ascoli Piceno, Italy

E-mail: [mariano.pierantozzi@unicam.it](mailto:mariano.pierantozzi@unicam.it)

**Abstract.** The values of thermal conductivity  $\lambda$  at different temperatures for organic and inorganic compounds in the liquid phase is essential in the study of numerous processes, but experimental data are frequently not available with acceptable reliability or not available at all, since rigorous theoretical or semi-theoretical models of the liquid state are usually of poor practical use for engineering purposes. The Artificial Neural Network (ANN) approach is a very powerful tool and it can be a good indicator of the lowest limit achievable with a selected database and with a selected set of inputs. This study investigates the applicability of the ANN as an efficient tool for the prediction of pure organic compounds' thermal conductivity of three important families such as alkanes, ketones and silanes, for a wide range of temperatures. The families of n-alkanes, ketones and silanes were chosen to verify the general reliability of the proposed method when used in large temperature ranges for very different organic families, above all the silanes (compounds containing silicon), whose liquid thermal conductivity is experimentally investigated in very few cases. This method appears to be successful: in all reduced temperature range, along or near the saturation line, the average absolute deviations between calculated and experimental thermal conductivity data are 0.19% and the maximum absolute ones 2.44%

## 1. Introduction

Recently our research group focused its attention on the study of some important thermo-physical properties [1–17]. One of the most important of them is thermal conductivity. The values of the thermal conductivity of liquids are required in several phenomena, but its experimental values at different temperatures are often not available with acceptable reliability or sometimes not available at all; theoretical or semi-theoretical models of the liquid state (“gas-like” or “solid-like” models) are useless or of poor practical use for engineering purposes, either for the errors they finally lead to, or for the excessive mathematical difficulties.

On a microscopic scale the liquids are obviously characterized by a potential function determining the energy transfer mechanisms, but the different models appeared in the scientific literature generally do not allow to find reliable values for thermal conductivity, and empirical or semi-empirical correlations are usually necessary for many practical or engineering purposes. In using these correlations, a reasonable equilibrium has to be reached between the simplicity of the method and the accuracy of the values of the estimated thermal conductivity.

The thermal conductivity of liquids usually decreases with the increase of temperature, with the exception of some compounds, for example water and some aqueous solutions. In the range from the normal melting point to the normal boiling point and over, the thermal conductivity dependence on the



temperature is usually almost linear, but this behavior near the critical point dramatically ceases and the critical point represents a singularity.

From a theoretical point of view [18, 19], the thermal conductivity of liquids depends upon temperature and density as sum of three contributions: the “dilute gas contribution”, the “excess contribution” and the “critical enhancement contribution”; the density dependence is usually substituted by pressure dependence because the pressure variations are negligible up to 3-4 MPa, and in this range it is acceptable to express thermal conductivity as a function of temperature only. In this work a suitable equation for the liquid phase is proposed linking liquid thermal conductivity directly with temperature. In a recent past [4], among the different organic families, n-alkanes, ketones and silanes were chosen as a test of the proposed estimation method. In this paper, the method is extended to three very different families: n-alkanes, ketones and silanes. The results are compared with nine of the best empirical or semi-empirical equations proposed in the scientific and technical literature.

In order to develop an acceptable comparison between estimated and experimental thermal conductivity data, the thermal conductivity values (experimental, smoothed and predicted) available from DIPPR801 [20] database for the n-alkanes, ketones and silanes are analyzed. During the data collection, a fluid by fluid analysis was performed and only experimental or experimental&predicted data with claimed accuracy less than 10% were taken into account for the check of the proposed method and for the comparison with the other investigated methods.

## 2. The database used for the test of Artificial Neural Network

Since reliable experimental thermal conductivity data of liquids available in literature are due to different authors who use different apparatuses at different temperatures (and, obviously, with different accuracies), a valid check would be developed by disposing of a unique collection of experimental thermal conductivity data. A reliable and updated source of thermal conductivity values can be found in the DIPPR801 database [20], where experimental, predicted and smoothed data are reported. The DIPPR 801 database collects data from a wide range of sources and considers them critically, giving quality codes for all data points. The DIPPR801 database was chosen as the source of the thermal conductivity data because the database satisfies the following requirements: the thermal conductivity data are clearly indicated as experimental, predicted or experimental&predicted; the accuracy of the thermal conductivity data is clearly indicated; if experimental thermal conductivity data are not available, the used estimation method is clearly indicated with the claimed accuracy.

The data are collected for the three selected families of n-alkanes, ketones and silanes.

The choices of the authors, as extensively exposed in a previous work [4] concerning the families considered, were as follows:

- only experimental or experimental&predicted data for each fluid with claimed accuracy better than 10% were used in the check of the model, thus the predicted thermal conductivity data presented in DIPPR801 were not taken into account;
- the results obtained through the Artificial Neural Network (ANN) were compared with the results of other ten estimation methods: seven methods are proposed in DIPPR801 [21–29], while three methods were taken from the recent literature. [3, 5, 30]

The compounds taken into account were the following ones:

- n-alkanes: 23 investigated compounds;
- ketones: 14 investigated compounds;
- silanes: 18 investigated compound.

The check was developed exploring the reduced temperature range 0.30 to 0.80.

## 3. An artificial Neural Network

For the modelling of thermal conductivity of n-alkanes, ketones and silanes, the Wolfram Mathematica artificial neural network toolbox was employed. A neural network is a structure involving weighted interconnections among neurons, or units, which are most often nonlinear scalar transformations, but they

can also be linear. A neuron is structured to process multiple inputs, including the unity bias, in a nonlinear way, producing a single output. Specifically, all inputs to a neuron are first augmented by multiplicative weights. These weighted inputs are summed and then transformed via an activation function (also called neuron function).

The training goal is to find values of the parameters so that, for any input  $x$ , the network output  $\hat{y}$  is a good approximation of the desired output  $y$ . Training is carried out via suitable algorithms that tune the parameters so that input training data map well the corresponding desired outputs. These algorithms are iterative in nature, starting at some initial value for the parameter vector  $\theta$ , and incrementally updating it to improve the performance of the network.

The network is generally divided into layers. The input layer consists of just the inputs to the network. Then follows a hidden layer, which consists of any number of neurons, or hidden units, placed in parallel. The network output is formed by another weighted summation of the outputs of the neurons in the hidden layer. This summation on the output is called the output layer.

The required number of training data points and hidden layer neurons are the main goals of ANN modelling. They can be determined by the constructive approach [31]. A network that has only one hidden layer is able to approximate almost any type of nonlinear mapping [32].

Each neuron performs a weighted summation of the inputs, which then passes through a nonlinear activation function  $s$ . Mathematically, the functionality of a hidden neuron is described by:

$$s(a) = s\left(\sum_{j=1}^n w_j x_j + b\right) \quad (1)$$

where  $a$  is the overall weighted input of the neuron and the weights  $w_j$ ,  $b$  are symbolized with the arrows feeding into the neuron itself. For this feedforward network, a sigmoid function was employed as the activation function:

$$s(a) = \frac{1}{1+e^{-a}} \quad (2)$$

The number of output neurons equals the number of outputs of the approximation problem. The output of this network is given by:

$$\hat{y} = g(\theta, x) = g\left(\sum_{i=1}^{nh} w_i s\left(\sum_{j=1}^n w_{i,j} x_j + b_i\right) + b_{out}\right) \quad (3)$$

where  $n$  is the number of inputs to the  $i^{\text{th}}$  neuron,  $nh$  is the number of neurons in the hidden layer, and  $b_{out}$  is the output bias. In this work, the output activation function  $g$  was chosen to be linear as this is a convenient and sufficient choice for interpolation problems.

The parameters of the network model are represented collectively by the parameter vector  $\theta$ . In general, the neural network model will be represented by the compact notation  $g(\theta, x)$ . The size of the input and output layers are defined by the number of inputs and outputs of the network and, therefore, only the number of hidden neurons has to be specified when the network is defined.

Keeping the number of hidden layers fixed, it is possible to modulate the network by changing the number of hidden neurons in each layer. In this way, we tested each time the network with a different number of neurons trying to limit the error produced by the model. Too few neurons in the hidden layer prevent the network from better fitting the experimental values and approximate points maintaining a low deviation. On the other hand, too many neurons lead to a network that has a very good response when it is tested with the training points, but the structure of this network is too rigid with the provided values.

Often it is more convenient to use the *RMSE* when evaluating the quality of a model during and after training, because it can be compared with the output signal directly. Different neural networks were compared adopting the Levenberg-Marquardt algorithm [33] using their Root Mean Square Errors (*RMSEs*), defined as follows:

$$RMSE = \sqrt{\frac{1}{N} \sum_{i=1}^N (y_i - g(\theta, x_i))^2} \quad (4)$$

where  $N$  is the number of data points.

When the network is trained with new data there is the risk of committing unacceptably large errors. These problems, occurring during the neural network training, are referred to as overfitting. To avoid and overcome this overfitting problem, it is possible to divide the data points into training, validation and test data.

Therefore, before the trained network is accepted, it should be validated. Roughly, this means running a number of tests to determine whether the network model meets certain requirements. In this case, it was decided to split the database into three parts: one that comprises 70% of the data, which were used for the “training”, a second which employs 20% of the data, which were used to perform the “validation” test, and a third which employs 10% of the data which were used for the “test” carried out to investigate the prediction capability and validity of the obtained model. In all cases, data were randomly chosen within the database.

Figure 1 illustrates a diagram of a one-hidden-layer feedforward network adopting the following inputs: experimental reduced temperature,  $T_r$ , the molecular weight  $M$ , and the acentric factor,  $\omega$ . In particular, the acentric factor is an important characterization of substances that was introduced by Pitzer in 1955 [34]. Pitzer came up with this factor by analyzing the vapor pressure curves of various pure substances [35]. Table 1 contains the molecular weight and the acentric factor for all the fluids taken into account.

The output is thermal conductivity,  $\lambda$ . Each arrow in the figure symbolises a parameter in the network. In summary, the selected ANN architecture includes three input parameters ( $T_r$ ,  $M$ ,  $\omega$ ), one hidden layers with 37 neurons, and a output neuron giving the thermal conductivity value for each fluid and each temperature. The values for the weights and bias for each neuron are given in Table 2 and 3.

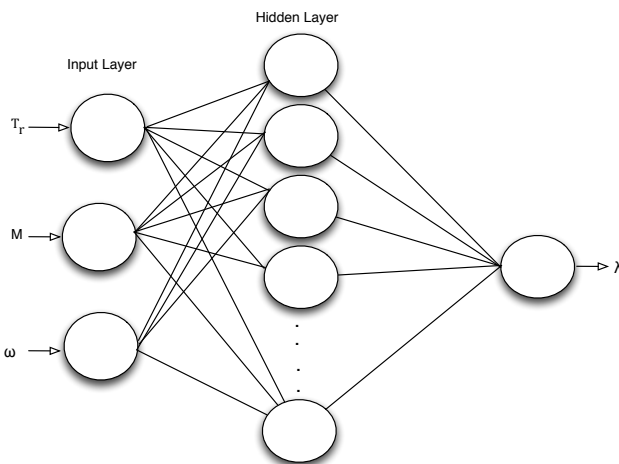


**Figure1.** Schematic diagram of the ANN model. Inputs:  $T_r$ , reduced temperature,  $M$  molecular weight,  $\omega$  acentric factor. Output:  $\lambda$  thermal conductivity

In order to compare the equations, deviations were calculated as follows:

$$AAD = \left| \frac{\lambda_{exp} - \lambda_{calc}}{\lambda_{exp}} \right| \cdot 100 \quad (5)$$

Figure 2 illustrates the  $AAD$  for the training, validation and test, and the overall set of data obtained for various neural network configurations with one hidden layer, achieved after 1000 iterations during the modeling of the thermal conductivity of n-alkanes, ketones and silanes. From the figure it is evident that, as expected,  $AAD$  decreases with the increase of the number of neurons and that a good configuration is reached when the number of neurons in the hidden layer is 37. This configuration was selected as the best network architecture.

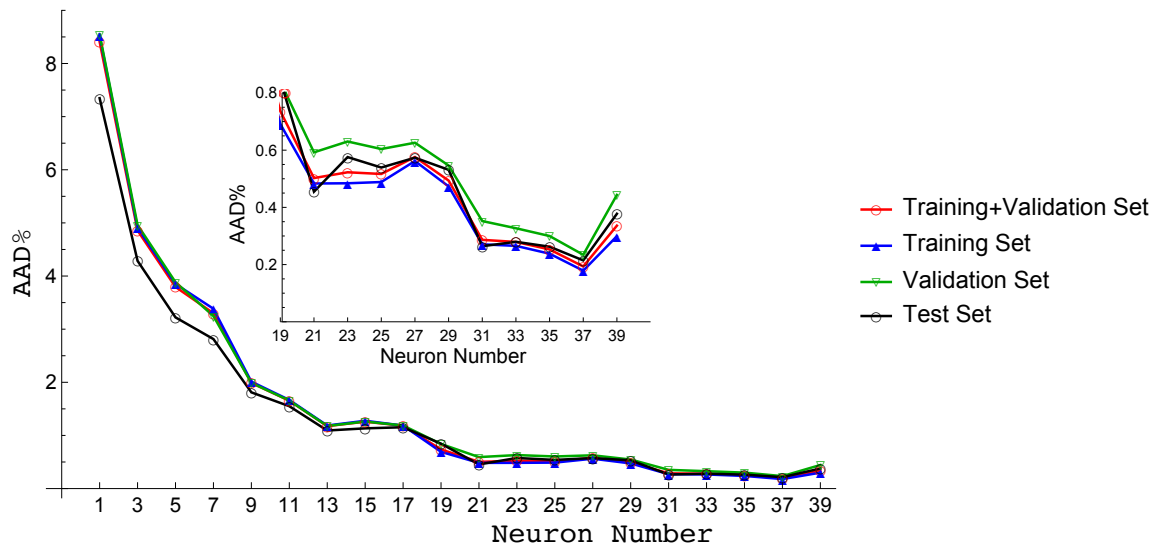


**Figure 2.** Absolute average percent deviation between data collected and ANN results vs number of neurons in hidden layer

The AADs for the proposed ANN are reported in Table 1.

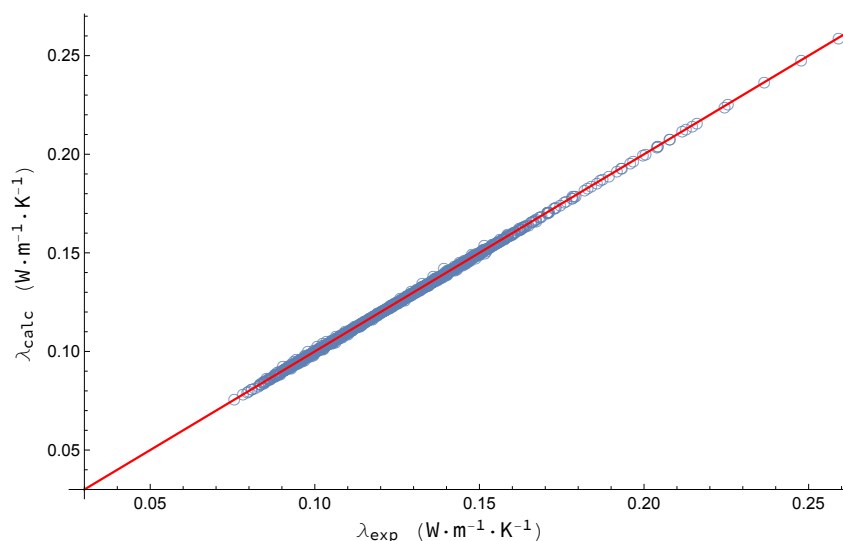
#### 4. Comparison between the results obtained through the proposed method (9) and the results obtained through different equations appeared in literature

Together with the methods from the literature and those proposed in DIPPR810 [5,8,9,17-24], two additional methods are taken into account [25,26]. All the methods, even if already appeared in [37], are shortly illustrated below for a convenient comparison.

Tables 1 shows the results of the comparison between the ANN model proposed by the authors and the correlations proposed in the literature by the authors indicated in the same Table for the n-alkanes, ketones and silanes, respectively.

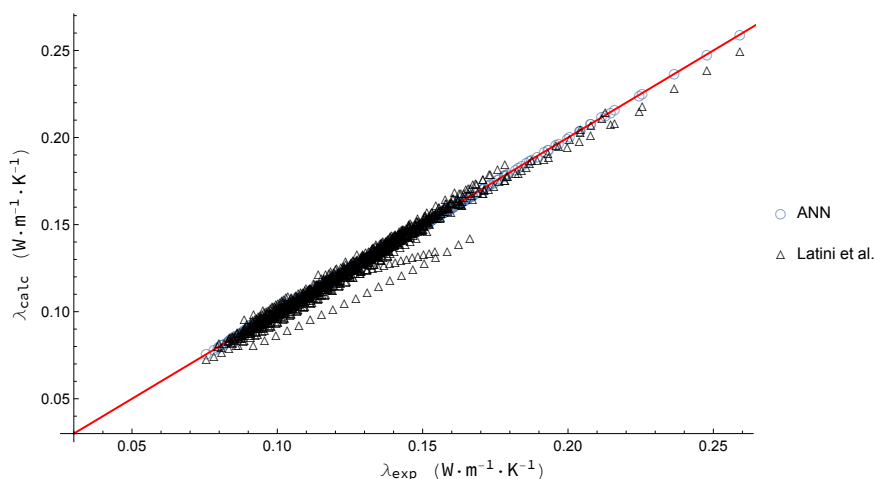
The blank spaces indicate that the estimation method is not acceptable for the corresponding compound.

Fig. 3 shows the calculated thermal conductivity values versus the ones in the database. As can be seen, there are not significant disagreements in the data considered.



**Figure 3.** Calculated thermal conductivity values versus all the values in the datasets when the selected ANN architecture is used.

In order to clearly show the improvement obtained with the use of the ANN with respect to the best corresponding-states model, Fig. 4 shows the calculated and dataset values for the proposed ANN and for the Latini et al. model [3]. As can be seen, the corresponding-state model cannot adequately reproduce a significant number of data. Some excessive over-predictions and under-predictions are clearly obtained.



**Figure 4.** Calculated thermal conductivity values versus values in the datasets when the selected ANN model and the Latini et al. [3] corresponding-state model are used

Fig. 5 shows the deviations values versus temperature. As can be seen, only a very few number of data give deviations values higher than 2%, in fact except very few points, residuals are well within  $\pm 2.0$   $W \cdot (m \cdot K)^{-1}$ .

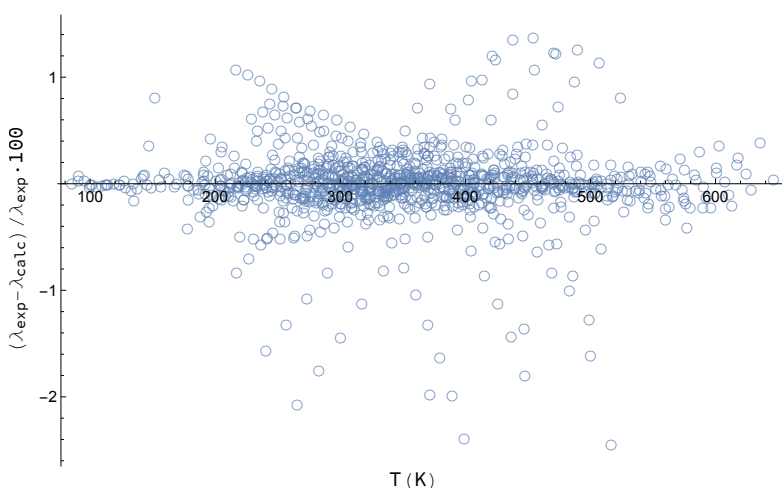


**Figure 5.** Deviations values for each dataset obtained by using the selected ANN architecture

## 5. Conclusions

In this paper a multilayer perceptron neural network are proposed to thermal conductivity of three important chemical families: ketones, alkanes and silanes. After checking different architectures and



different input variables, the ANN model giving the better results includes three input properties for each fluid ( $T_r$ ,  $M$ ,  $\omega$ ), one hidden layers with 37 neurons, and a output neuron.

The model was validated, trained and tested for a wide set of data, showing that the accuracy of the neural network model is higher than the accuracy of the methods proposed in the literature. This selected model can reproduce the data with an overall AAD value of 0.19%, and a maximum AAD value of 2.44%

For the sake of comparison, we have shown that the presently available corresponding-states models cannot reproduce these data with AAD below 1%. The proposed ANN model can be considered then as a very accurate tool to reproduce the currently available thermal conductivity data for the considered families and even for prediction purposes. Needed input properties, bias, and weights values are given in Table 2 and 3.

## References

- [1] Di Nicola G, Coccia G, Malvagi L, Pierantozzi M 2017 *J. Thermophys. Heat Transf.* 1–9.
- [2] Khosharay S, Khosharay K, Di Nicola G, Pierantozzi M 2017 *Phys. Chem. Liq.* 1–17.
- [3] Latini G, Di Nicola G, Pierantozzi M 2017 *Phys. Chem. Liq.* 1–19.
- [4] Latini G, Di Nicola G, Pierantozzi M 2016 *Fluid Phase Equilib.* **427** 488–497.
- [5] Di Nicola G, Pierantozzi M, Petrucci G, Stryjek R 2016 *J. Thermophys. Heat Transf.* **30** 651–660.
- [6] Di Nicola G, Coccia G, Pierantozzi M 2016 *Fluid Phase Equilib.* **417** 229–236.
- [7] Di Nicola G, Coccia G, Pierantozzi M, Falone M 2016 *Int. J. Refrig.* **68** 242–251.
- [8] Di Nicola G, Coccia G, Pierantozzi M 2016 *Fluid Phase Equilib.* **418** 88–93.
- [9] Di Nicola G, Pierantozzi M 2015 *Fluid Phase Equilib.* **389** 16–27.
- [10] Latini G, Di Nicola G, Pierantozzi M 2014 *Energy Procedia* **45** 616–625.
- [11] Di Nicola G, Pierantozzi M 2014 *J. Therm. Anal. Calorim.* **116** 129–134.
- [12] Di Nicola G, Falone M, Pierantozzi M, Stryjek R 2014 *Ind. Eng. Chem. Res.* **53** 13804–13809.
- [13] Di Nicola G, Ciarrocchi E, Coccia G, Pierantozzi M 2014 *Int. J. Refrig.* **45** 168–176.
- [14] Di Nicola G, Ciarrocchi E, Pierantozzi M, Stryjek R 2014 *J. Therm. Anal. Calorim.* **116** 135–140.
- [15] Di Nicola G, Pierantozzi M 2013 *Int. J. Refrig.* **36** 562–566.
- [16] Mulero Á, Pierantozzi M, Cachadiña I, Di Nicola G 2017 *Fluid Phase Equilib.* **449** 28–40.
- [17] Pierantozzi M, Nicola G Di, Latini G, Coccia G *Phys. Chem. Liq.* **0** 1–18.
- [18] Assael MJ, Trusler JPM, Tsolakis TF 1996 *Thermophysical Properties of Fluids.*
- [19] Assael MJ, Charitidou E, Wakeham WA 1989 *Int. J. Thermophys.* **10** 779–791.
- [20] The DIPPR Information and Data Evaluation Manager for the Design Institute for Physical Properties 2016.
- [21] Sastri SRS, Rao KK 1999 *Chem. Eng. J.* **74** 161–169.
- [22] Missenard A 1965 *Conductivité thermique des solides, liquides, gaz et de leurs mélanges.*
- [23] Riedel L 1951 *Chemie Ing. Tech.* **23** 321–324.
- [24] Reid RC, Prausnitz JM, Poling BE 1987 *The Properties of Gases and Liquids* (McGraw-Hill)
- [25] Baroncini C, Di Filippo P, Latini G, Pacetti M 1981 *Int. J. Thermophys.* **2** 21–38.
- [26] Poling BE., Prausnitz JM, O apos Connell JP 2007 *Exp. Therm. Fluid Sci.* **1** 1–803.
- [27] Nagvekar M, Daubert TE 1987 *Ind. Eng. Chem. Res.* **26** 1362–1365.
- [28] Robbins L, Kingrea C 1962 *Hydrocarb. Process. Pet. Refinerining* **41** 133–136.
- [29] Pachaiyappan V, Ibrahim S, Kuloor N 1967 *Chem. Eng.* **74** 140–144.
- [30] Gharagheizi F, et al. 2013 *AIChE J.* **59** 1702–1708.
- [31] Haykin SS 1999 *Neural Networks: A Comprehensive Foundation* (Prentice Hall)
- [32] Cybenko G 1989 *Math. Control. Signals, Syst.* **2** 303–314.
- [33] Marquardt DW 1963 *J. Soc. Ind. Appl. Math.* **11** 431–441.
- [34] Pitzer KS, Lippmann DZ, Curl RF, Huggins CM, Petersen DE 1955 *J. Am. Chem. Soc.* **77** 3433–3440.
- [35] Pitzer KS 1977 Origin of the Acentric Factor, pp 1–10.
- [36] Missenard A 1965 *Conductivité thermique des solides, liquides, gaz et de leurs mélanges* (Eyrolles, Paris).
- [37] Latini G, Di Nicola G, Pierantozzi M 2016 *Fluid Phase Equilib.* **427** 488–497.



**Table1.** Dataset of the fluids considered in the present work and absolute relative deviations (*AAD*) for each fluids for the ANN and the comparison with literature models taken into account.

Fluid	Molecular Weight [kg/kmol]	Acentric Factor	Present work	Latini et al. [3]	Sastri-Rao [20]	Missenard [21]	Sato-Riedel [25]	Latini et al [24]	Nagvekar-Daubert [26]	Robbins-Kingrea [27]	Pachaiyappan et al [28]	Gharagheizi et al [29]	Di Nicola et al [5]
methane	16.04	0.01	0.11	2.3	28.5	26.3	48.8	55.8	-	2.6	58.3	13.5	7.6
ethane	30.07	0.1	0.04	2.8	11.1	56.5	17.9	42.1	29.8	18.2	36.9	11.8	12.8
propane	44.1	0.15	0.05	3.8	34	14.6	25.3	23.8	9.2	17.6	17.2	13.4	5.9
n-butane	58.12	0.2	0.07	3.2	46.1	5.5	19.4	15.9	3.8	9.4	9.8	10.4	5.1
n-pentane	72.15	0.25	0.18	0.7	56.2	4.5	16	8.8	2.3	11.6	11.9	9.2	5
n-hexane	86.18	0.3	0.17	1.9	61.5	3.1	11.4	5.1	3.7	9.1	13.7	6.2	3.1
n-heptane	100.2	0.35	0.31	1.2	63.2	1.5	6.4	3.2	4.6	10.1	16.1	4.8	1.4
n-octane	114.23	0.4	0.87	0.5	69.5	1.9	3.6	1.7	5.4	5.8	22.9	4.3	1.7
n-nonane	128.26	0.44	0.46	1.1	72.4	1	0.9	1.1	5.4	7	25.9	4	0.9
n-decane	142.28	0.49	0.64	1.2	77.4	1.2	1.8	2.7	5.9	4.5	30.5	3.4	1.7
n-undecane	156.31	0.53	0.23	1.2	79.7	0.9	4.4	3.4	5.7	5.1	32.7	3.7	1.3
n-dodecane	170.33	0.57	0.26	1	83.2	1	6.2	4.3	5.7	3.3	35.9	3.6	1.8
n-tridecane	184.36	0.62	0.13	1.1	85.3	0.6	8.2	4.5	5.2	6.5	37	3.9	1.8
n-tetradecane	198.39	0.66	0.06	1.1	87.9	0.6	9.9	5.2	5.3	6.8	39.8	3.7	1.6
n-pentadecane	212.41	0.7	0.08	1.9	87.9	1.4	12.4	4.3	3.9	6.8	39.8	4.8	1.1
n-hexadecane	226.44	0.73	0.11	1.5	91.3	1.2	13.2	5.2	4.5	8.6	42.7	4.1	2
n-heptadecane	240.47	0.77	0.31	1.4	94.9	1.4	13.7	6.2	5.1	9.7	45.3	3.1	4.5
n-octadecane	254.49	0.8	0.17	1.1	95.2	2.2	15.6	5	4.1	12.1	45.3	4	4.3
n-nonadecane	268.52	0.84	0.12	0.8	97.8	3.7	16.3	5.3	4.4	12.7	47.3	3.5	5.8
n-eicosane	282.55	0.91	0.05	2.5	95.7	7.6	18.8	3.3	3.7	15	44.4	5.3	5.5
n-heneicosane	296.57	0.94	0.11	4	95.2	7.7	20.3	2.6	3.6	15.7	44.1	5.9	5.1
n-docosane	310.6	0.97	0.04	4.1	94.1	8.7	22.2	2	3.8	16.9	43	7.1	4
n-tricosane	324.63	1.03	0.13	2.7	94.6	9.5	23.3	1.8	4.1	19.2	43	7.4	5.6
n-tetracosane	338.65	1.07	0.06	0.7	93.7	10.7	24.9	2.5	4.8	21.5	41.8	8.4	5.8
acetone	58.08	0.31	0.05	1.8	31.5	5.2	2.3	9.7	7.2	12.1	4.9	8.8	13.8
methyl ethyl ketone	72.11	0.32	0.02	1.5	46.4	7.2	4.1	2.4	13.4	26.4	13.5	3.3	4.6
2-pentanone	86.13	0.34	0.17	2.6	59.9	3.4	1.6	3.9	17.8	19.9	15.7	5	4.6
3-pentanone	86.13	0.34	0.13	0.9	58.4	6.1	1.6	2	21.7	15.9	16.1	6	6.2
2-hexanone	100.16	0.38	0.32	0.4	69.5	4.2	0.9	7.8	22.5	14.9	19	8.8	5.6
2-heptanone	114.19	0.42	0.36	1	78.8	5.4	1.4	11.5	27	12.2	22.4	3	1.1
3-heptanone	86.13	0.34	0.15	0.5	79.4	5.6	3.1	9.3	32.1	11	25.7	3.2	6.7
4-heptanone	114.19	0.41	0.89	3.2	75.6	4.6	5.5	5.8	29.1	10.5	22.8	5.7	4.7
2-octanone	128.21	0.46	0.31	2.7	86.4	4.9	4.1	12.9	29.5	6.7	25.8	3.2	1.1
2-nonanone	142.24	0.49	0.96	3.1	93.1	6.7	5.2	15.3	32.3	8.4	28	1.8	2.3
5-nonanone	142.24	0.51	0.52	0.6	92.3	5.4	5.6	12.5	36.6	7.9	28.1	3.4	2.2
cyclopentanone	84.12	0.29	0.11	3.9	57.2	8.5	3.4	-	19.8	18.6	30.9	1.7	6.9
cyclohexanone	98.14	0.4	0.18	1.7	70.9	3.9	3.8	-	28.5	40.3	38.2	3.8	4.9
acetophenone	120.15	0.4	0.1	1.8	76.7	5.4	9.4	2.2	57.2	21	28.7	1.3	6.9

Methyl trichlorosilane	149.48	0.24	0.11	3.1	-	26.6	29.9	-	-	-	-	35.8	29.8
Dichlorodiethylsilane	157.11	0.32	0.11	0.8	-	19.6	19	-	5.6	-	-	19.5	17.9
Vinyltrichlorosilane	161.49	0.28	0.14	14.1	-	23.4	22.7	-	78.9	-	-	26.4	23.2
Phenyltrichlorosilane	211.55	0.4	0.26	4.9	-	16.6	16.9	-	2.7	-	97.9	7.8	9.2
Diphenyldichlorosilane	253.2	0.43	0.11	5	-	5.7	7.7	-	141.8	-	107.5-	14.6	4.4
Hexamethylcyclotrisiloxane	222.46	0.5	0.06	4.7	-	2.6	15.1	-	-	-	-	16.3	10.1
Octamethylcyclotetrasiloxane	296.62	0.55	0.12	0.2	-	2.7	19.5	-	-	-	-	15.3	10.7
Decamethylcyclopentasiloxane	370.77	0.64	0.21	1.4	-	14.1	31.1	-	-	-	-	22	21.7
Dodecamethylcyclohexasiloxane	444.92	0.71	0.08	5.3	-	24.1	37.1	-	-	-	-	24.6	26
Hexadecamethylcyclooctasiloxane	593.23	0.88	0.04	1.4	-	31	43.1	-	-	-	-	25.6	27.7
Hexamethyldisiloxane	162.38	0.41	0.17	2.5	-	9.8	8.5	-	-	-	-	6.8	9.6
Octamethyltrisiloxane	236.53	0.54	0.3	1.4	-	6.7	7.8	-	-	-	-	8.2	9.1
Decamethyltetrasiloxane	310.69	0.66	0.06	3.2	-	7.1	15	-	-	-	-	8.9	8.2
Dodecamethylpentasiloxane	384.84	0.68	0.07	2.1	-	16.3	23.1	-	-	-	-	12	9.6
Tetradecamethylhexasiloxane	458.99	0.8	0.08	6.4	-	38.3	45.9	-	-	-	-	15.6	12.2
Hexadecamethylheptasiloxane	533.15	0.89	0.07	0.6	-	29.8	35.2	-	-	-	-	17.7	15
Methyl silicate	152.22	0.44	0.05	0.8	-	28.4	29.9	-	85.5	-	-	33	26
Tetraethoxysilane	208.33	0.63	0.12	2.9	-	14.2	20.8	-	65.6	-	-	20.6	7.7

**Table 2.** Hidden layer weights

Hidden neurons	bias	Tr	Mass	Acentric factor
Neurons				
1	0.32	-4.41	5.65	-4.41
2	-8.61	-0.02	34.52	21.49
3	19.66	-0.76	-20.12	-26.47
4	-12.56	0.17	22.76	43.27
5	15.31	1.05	-14.75	-0.98
6	-5.66	0.19	43.06	3.62
7	10.11	-0.07	-52.58	-2.51
8	4.09	-0.27	42.95	-43.39
9	4.16	-0.64	37.79	-37.19
10	18.87	0.33	-19.43	-1.74
11	16.64	0.08	6.91	-43.33
12	8.55	-0.24	49.42	-59.57
13	26.90	-0.21	-26.36	-7.64
14	3.17	-0.01	-41.58	9.08
15	-19.83	1.04	11.51	38.43
16	-5.25	-0.14	-52.33	38.98
17	14.87	-21.78	-1.62	8.33
18	14.12	-0.31	-25.21	-2.69

19	8.69	0.30	-29.17	-18.43
20	-7.62	0.49	20.56	-4.63
21	4.27	0.10	1.27	-6.27
22	-6.87	-0.62	14.96	34.81
23	4.27	1.92	-8.64	-1.12
24	-11.40	-0.22	11.12	22.57
25	-8.30	-0.36	3.80	24.48
26	-3.76	-0.60	4.71	1.86
27	-9.59	0.36	35.03	13.27
28	-11.50	0.32	-45.52	63.01
29	-15.39	-0.98	13.96	39.93
30	2.64	-6.43	-1.66	-6.79
31	14.41	-0.32	-16.43	-8.09
32	2.22	0.07	43.18	-28.50
33	9.21	-0.18	-12.57	-1.08
34	0.10	0.39	-5.91	-20.84
35	19.03	-0.53	51.78	-86.00
36	18.59	-22.21	-0.81	7.41
37	0.10	0.02	58.92	-33.71

**Table 3.** Output layer weights

Output of Neurons

1	-31.12
2	-0.22
3	-0.56
4	-0.44
5	-0.42
6	-0.26
7	-27.46
8	-0.89
bias	29.77